

Novel binuclear copper(II) complexes of di-2-pyridyl ketone *N*(4)-methyl, *N*(4)-phenylthiosemicarbazone: Structural and spectral investigations

Varughese Philip ^a, V. Suni ^a, Maliyeckal R. Prathapachandra Kurup ^{a,*},
Munirathinam Nethaji ^b

^a Department of Applied Chemistry, Cochin University of Science and Technology, Kochi 682 022, Kerala, India

^b Department of Inorganic and Physical Chemistry, Indian Institute of Science, Bangalore 560 012, India

Abstract

Four binuclear complexes [Cu(dptsc)Cl]₂ · 3H₂O (**1**), [Cu(dptsc)Br]₂ (**2**), [Cu(dptsc)(μ-N₃)₂] (**3**) and [Cu(dptsc)(NO₃)₂] · H₂O (**4**) (where Hdptsc = di-2-pyridyl ketone *N*(4)-methyl, *N*(4)-phenylthiosemicarbazone) have been synthesized and physicochemically characterized. Each Cu(II) atom in the monomeric unit exists in a penta-coordinate environment. The molecular structures of [Cu(dptsc)Br]₂ and [Cu(dptsc)(μ-N₃)₂] are resolved by single-crystal X-ray diffraction studies. Both the crystals are centrosymmetric dimers where each ligand unit coordinates through one of the pyridyl nitrogens, azomethine nitrogen and thiolate sulfur to Cu(II). A distorted square pyramidal geometry is observed around Cu(II) for both the complexes, where the N(2) nitrogen of the second ligand unit coordinates to the first Cu(II) center in compound **2** and N(6) nitrogen of the azido group bridges both the Cu(II) centers in compound **3**. Spectral characterization corroborate the structural studies.

Keywords: Di-2-pyridyl ketone; Thiosemicarbazone; Cu(II) thiosemicarbazone complex; Crystal structure

1. Introduction

The ability of nitrogen and/or sulfur based donors to stabilize reduced and oxidized forms of copper(II) has sparked interest in their bioinorganic systems [1]. Thiosemicarbazones and their metal complexes are nowadays widely explored owing to their versatile biological activity and prospective use as drugs [2]. The potential anticancer, chemotherapeutic and superoxide dismutase-like activity of copper complexes with various thiosemicarbazones were first reported during 1950s [3,4]. Thereafter, a great variety of biological properties rang-

ing from anticancer [5], antitumor [6], antibacterial [7], antifilarial [8] and antiviral [9] activities were explored with thiosemicarbazones, while the Cu(II) derivatives of bis(thiosemicarbazone) ligands served as radiopharmaceuticals [10] and revealed hypoxic selectivity [11]. For the past decade, we have been in constant pursuit of the synthesis, structural characterization and biological studies of a variety of substituted and unsubstituted thiosemicarbazones with different combinations of the aldehydes/ketones, with the aim to correlate their structural features with chelating ability and biological activity [12–17]. However, there are only few previous reports on di-2-pyridyl ketone thiosemicarbazones [18–22], and recently we have reported the synthesis and unique structural features of di-2-pyridyl ketone *N*(4), *N*(4)-(butane-1,4,diyl)thiosemicarbazone [23] and its Ni(II)

* Corresponding author. Tel.: +91 484 2575804; fax: +91 484 2577595.

E-mail address: mrp@cusat.ac.in (M.R. Prathapachandra Kurup).

complexes [24]. In this paper, we report the spectral characteristics of four copper(II) complexes derived from di-2-pyridyl ketone *N*(4)-methyl-*N*(4)-phenylthiosemicarbazone (Hdptsc) (Fig. 1). The crystal structures of two complexes formulated as $[\text{Cu}(\text{dptsc})\text{Br}]_2$ (**2**) and $[\text{Cu}(\text{dptsc})(\mu\text{-N}_3)]_2$ (**3**) are also described.

2. Experimental

2.1. Materials

Di-2-pyridyl ketone (Fluka) was used as received. $\text{CuCl}_2 \cdot 2\text{H}_2\text{O}$, CuBr_2 , $\text{Cu}(\text{OAc})_2 \cdot \text{H}_2\text{O}$, $\text{Cu}(\text{NO}_3)_2 \cdot 2.5\text{H}_2\text{O}$ and NaN_3 were commercial products of higher grade (Merck) and solvents were purified according to standard procedures. Elemental analyses were carried out using a Heraeus Elemental Analyzer and the molar conductance measurements of the complexes were carried out in DMF solvent at $28 \pm 2^\circ\text{C}$ on a Century CC-601 digital conductivity meter with dip type cell and platinum electrode. Approximately 10^{-3}M solutions were used. The magnetic susceptibility measurements were made using a simple Gouy balance at room temperature using mercury tetrathiocyanatocobaltate(II), $\text{Hg}[\text{Co}(\text{NCS})_4]$ as calibrant. Infrared spectral measurements were done on a Shimadzu DR 8001 series FTIR instrument using KBr pellets for spectra in the region $4000\text{--}400\text{ cm}^{-1}$, and far IR spectra were recorded using polyethylene pellets in the $500\text{--}100\text{ cm}^{-1}$ region on a Nicolet Magna 550 FTIR instrument. An Ocean Optics SD 2000 Fiber Optic Spectrometer was used to measure solid-state reflectance spectra in the range $200\text{--}900\text{ nm}$. ^1H NMR spectra were recorded using AMX 400 MHz FT-NMR Spectrometer with CDCl_3 as solvent and TMS as the internal standard. EPR spectral measurements were carried out on a Varian E-112 X-band spectrometer using TCNE as standard.

2.2. Synthesis of ligand

The ligand, Hdptsc was synthesized as reported earlier [24]. A solution of di-2-pyridyl ketone (1.84 g,

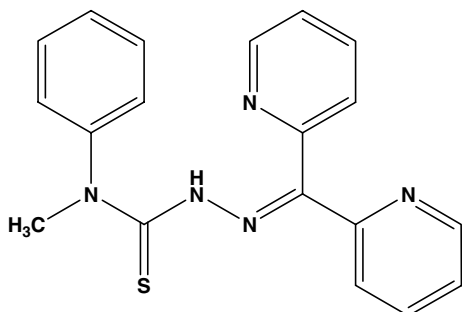


Fig. 1. Structure of Hdptsc.

10 mmol) in 5 ml methanol was treated with *N*(4)-methyl, *N*(4)-phenylthiosemicarbazide (1.81 g, 10 mmol) in 25 ml methanol and refluxed for 2 h. On slow evaporation at room temperature, bright yellow crystals of Hdptsc separated out. These crystals were collected, washed with methanol and dried over P_4O_{10} in vacuo.

2.3. Synthesis of $\text{Cu}(\text{dptsc})\text{Cl}_2 \cdot 3\text{H}_2\text{O}$ (**1**)

Methanolic solutions of Hdptsc (0.347 g, 1 mmol) and $\text{CuCl}_2 \cdot 2\text{H}_2\text{O}$ (0.171 g, 1 mmol) were mixed and heated under reflux for 2 h. Dark blue-green crystals of complex **1** were obtained, which were separated, washed with methanol followed by ether and dried over P_4O_{10} in vacuo. Yield: 0.25 g (52%).

2.4. Synthesis of $[\text{Cu}(\text{dptsc})\text{Br}]_2$ (**2**)

Hdptsc (0.347 g, 1 mmol) was dissolved in methanol (15 ml) and refluxed with a solution of CuBr_2 (0.223 g, 1 mmol) in 1:1 methanol–chloroform mixture. Blue crystals separated out, which were filtered, washed with methanol followed by ether and dried in vacuo. Colourless single crystals suitable for X-ray diffraction were grown by slow evaporation of a 1:1:1 solution of methanol, chloroform and dichloromethane of the complex. Yield: 0.175 g (33%).

2.5. Synthesis of $[\text{Cu}(\text{dptsc})(\mu\text{-N}_3)]_2$ (**3**)

$\text{Cu}(\text{OAc})_2 \cdot \text{H}_2\text{O}$ (0.199 g, 1 mmol) dissolved in methanol (15 ml) was added to Hdptsc (0.347 g, 1 mmol) and refluxed. NaN_3 (0.0651 g, 1 mmol) was then added to the solution and further refluxed for 3 h. Dark blue crystals of **3** separated out, which were collected and dried in vacuo. Single crystals for X-ray diffraction were grown by slow evaporation of a 1:1:1 solution of methanol, chloroform and dichloromethane of the complex. Yield: 0.35 g (56%).

2.6. Synthesis of $[\text{Cu}(\text{dptsc})(\text{NO}_3)]_2 \cdot \text{H}_2\text{O}$ (**4**)

A solution of $\text{Cu}(\text{NO}_3)_2 \cdot 2.5\text{H}_2\text{O}$ (0.233 g, 1 mmol) in a methanol–chloroform mixture (20 ml, v/v) was added to Hdptsc (0.347 g, 1 mmol) and refluxed for 2 h. The resulting crystals were washed with methanol, followed by ether and dried in vacuo. Yield: 0.35 g (65%).

2.7. X-ray crystallography

Single crystal X-ray diffraction measurements were carried out on a Bruker Smart Apex CCD diffractometer equipped with a fine-focused sealed tube. The unit cell parameters were determined and the data collections were performed using graphite-monochromated $\text{Mo K}\alpha$

Table 1
Elemental analyses, colours and molar conductivities of the Cu(II) complexes

Compound	Colour	Composition % (Found/Calc.)			λ_M^a	μ_{eff}^b (BM)
		Carbon	Hydrogen	Nitrogen		
[Cu(dptsc)Cl] ₂ · 3H ₂ O (1)	Blue	48.54 (48.30)	3.65 (4.05)	14.71 (14.82)	32	1.63
[Cu(dptsc)Br] ₂ (2)	Blue	46.63 (46.58)	3.32 (3.29)	14.35 (14.30)	27	2.24
[Cu(dptsc)(μ -N ₃) ₂ (3)	Blue	50.53 (50.49)	3.62 (3.57)	24.82 (24.79)	27	1.98
[Cu(dptsc)(NO ₃) ₂ · H ₂ O (4)	Blue	46.67 (47.44)	3.45 (3.56)	17.98 (17.47)	24	2.56

^a Molar conductivity, 10⁻³ M DMF at 298 K.

^b Magnetic susceptibility.

($\lambda = 0.71073 \text{ \AA}$) radiation. Both the crystals were found to be monoclinic with a $P2_1/c$ space group. Least square refinements of 17855 and 17083 reflections were done for compounds 2 and 3, respectively. The data collected were reduced using the SAINT program [25]. The trial structures were obtained by direct methods [26] using SHELXS-86, which revealed the position of all non-hydrogen atoms and refined by full-matrix least squares on F^2 (SHELXL-97) [27] and the graphic tool was DIAMOND for windows [28]. All non-hydrogen atoms were refined anisotropically, while the hydrogen atoms were treated with a mixture of independent and constrained refinements.

3. Results and discussion

3.1. Synthesis of complexes

Compounds 1, 2 and 4 were prepared by direct reaction between the ligand and the corresponding metal

salts, while compound 3 was prepared by the displacement of the acetate in Cu(OAc)₂ · H₂O by the azide ion. The complexes are mostly blue or blue-green coloured, as expected with thiosemicarbazone coordination, resulting from the ligand to copper charge transfer bands [29]. Elemental analyses (C, H, N) data (Table 1) of the complexes are consistent with the 1:1:1 ratio of metal:thiosemicarbazone:gegenion and also reveals that compounds 1 and 4 are hydrated. Conductivity measurements in DMF solution (10⁻³ M) indicate that all the complexes are non-electrolytes suggesting anionic coordination to the metal centre.

3.2. Crystal structures of [Cu(dptsc)Br]₂ and [Cu(dptsc)(μ -N₃)₂

Structural studies of compound 2 reveal a three-dimensional copper-thiosemicarbazone network consisting of two units of [Cudptsc] with a distorted square pyramidal geometry around Cu(II), with the basal plane

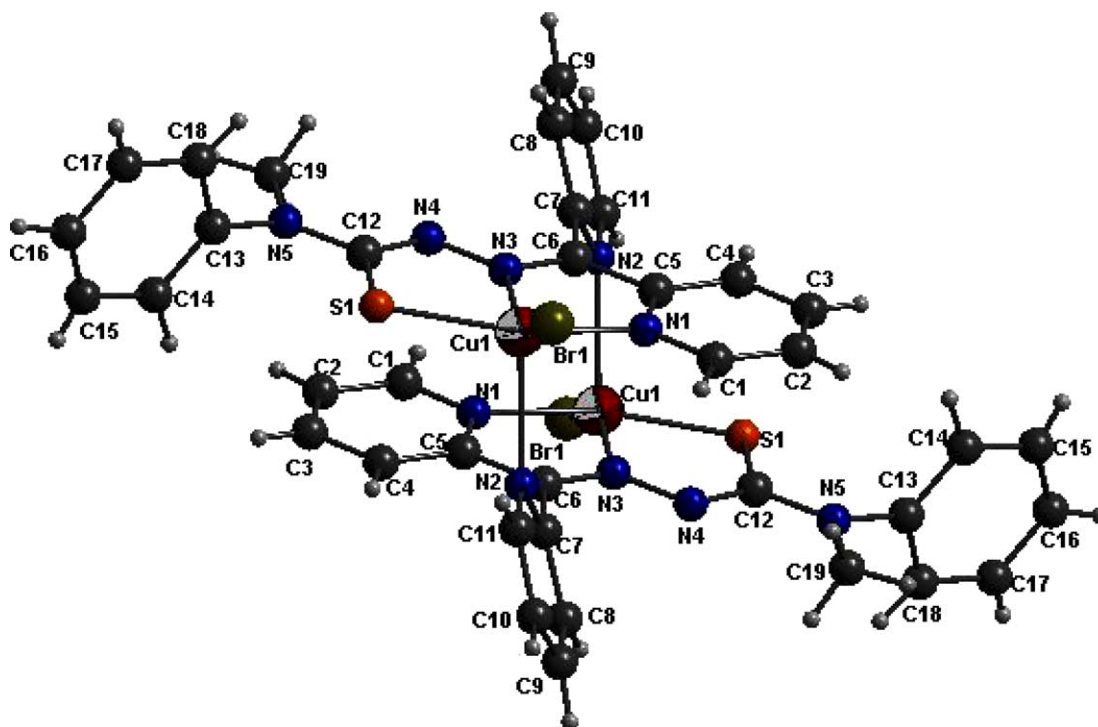


Fig. 2. Molecular structure of complex 2.

consisting of one of the pyridyl nitrogens, azomethine nitrogen, thiolate sulfur and the bromine atom, while the pyridyl nitrogen of the second ligand unit occupies the apical position. A labelled representation of **2** is depicted in Fig. 2 along with the structural data refinements (Table 2) and selected bond distances and angles (Table 3). The bite angles N(1)–Cu(1)–N(3) (80.05°), Br(1)–Cu(1)–N(1) (96.81°), Br(1)–Cu(1)–S(1) (95.22°) and S(1)–Cu(1)–N(3) (83.60°) also support the distortion from square pyramidal geometry. The basal plane consisting of N(1), N(3), Br(1), S(1) and Cu(1) shows a maximum mean deviation of -0.3411 \AA at N3. The Cu(II) atom is deviated at a distance of 0.3002 \AA out of the mean plane towards the apical position. The thiosemicarbazone moiety comprising of N(5), C(12), S(1), N(4) and N(3) atoms and the pyridyl ring, Cg(3), make dihedral angles of 18.73° and 18.58° , respectively, with the metal chelate CuN_2BrS square plane. The loss of the proton bound to N(4) in Hdptsc produces a negative charge, which is delocalized on the thiosemicarbazone moiety. Delocalization of electron density over the entire thiosemicarbazone moiety is evidenced by the little marginal change in the C(6)–N(3) and N(3)–N(4) bond distances in **2**, compared to

that of the uncomplexed thiosemicarbazone [30]. The bond distance S(1)–C(12) is longer and C(12)–N(4) is shorter than the corresponding values in the free ligand, which support thiolate formation in the ligand on complexation [31].

The structural pattern of the discrete binuclear complex, $[\text{Cu}(\text{dptsc})(\mu\text{-N}_3)]_2$ (**3**) is best viewed as two end-on $\mu_{1,1}$ -azido bridged quasi-square pyramids. Each Hdptsc unit acts as a tridentate chelate, coordinating through one of the pyridyl nitrogens, azomethine nitrogen and the thiolate sulfur to a single Cu(II) center which is involved in a $\mu_{1,1}$ -azido bridging to an identical coordination network, thus materializing a penta-coordinated environment (Fig. 3). The base of each distorted square pyramidal unit is occupied by N(1), N(3), N(6) and S(1) atoms, with the apical position occupied by the N(6) atom of the second azido group. Each azido ligand functions as an electron donor to the coordination network through an end-on azido bridging mode. The centrosymmetric nature of the structure is revealed by an inversion center with the two azido-bridged angles, Cu–N–Cu (92.94°) and N–Cu–N (87.06°), being the same in both the units. The intramolecular Cu–Cu distance is found to be 3.303 \AA and the axial Cu(1)–N(6)

Table 2
Crystal data, data collection and structure refinement parameters for $[\text{Cu}(\text{dptsc})\text{Br}]_2$ and $[\text{Cu}(\text{dptsc})(\text{N}_3)]_2$

Parameters	$[\text{Cu}(\text{dptsc})\text{Br}]_2$	$[\text{Cu}(\text{dptsc})(\text{N}_3)]_2$
Empirical formula	$\text{C}_{19}\text{H}_{16}\text{BrCuN}_5\text{S}$	$\text{C}_{19}\text{H}_{16}\text{CuN}_8\text{S}$
Formula weight (M)	489.88	452.00
Temperature, T (K)	293(2)	293(2)
Wavelength (Mo $K\alpha$) (\AA)	0.71073	0.71073
Crystal system	monoclinic	monoclinic
Space group	$P2_{1/c}$	$P2_{1/c}$
<i>Lattice constants</i>		
a (\AA)	9.029(4)	12.845(8)
b (\AA)	17.279(8)	12.512(7)
c (\AA)	13.217(6)	13.014(8)
α ($^\circ$)	90.00	90
β ($^\circ$)	97.228(8)	107.753(10)
γ ($^\circ$)	90.00	90.00
Volume, V (\AA^3)	2045.6(16)	1992(2)
Z	4	4
Calculated density, ρ (Mg m^{-3})	1.591	1.507
Absorption coefficient, μ (mm^{-1})	3.136	1.224
$F(0\ 0\ 0)$	980	924
Crystal size (mm)	$0.41 \times 0.13 \times 0.11$	$0.30 \times 0.12 \times 0.09$
θ Range for data collection	2.36–27.98	1.66–28.04
Limiting indices	$-11 \leq h \leq 11, -22 \leq k \leq 22, -17 \leq l \leq 16$	$-16 \leq h \leq 16, -16 \leq k \leq 16, -16 \leq l \leq 16$
Reflections collected	17 855	17 083
Unique reflections	4687 [$R_{\text{int}} = 0.0207$]	4682 [$R_{\text{int}} = 0.0265$]
Completeness to θ (%)	27.98 (99.2)	28.04 (97.1)
Maximum and minimum transmission	0.7242 and 0.3596	0.8978 and 0.7102
Refinement method	full-matrix least-squares on F^2	full-matrix least-squares on F^2
Data/restraints/parameters	4877/0/296	4682/0/326
Goodness-of-fit on F^2	1.025	1.074
Final R indices [$I > 2\sigma(I)$]	$R_1 = 0.0431, wR_2 = 0.1202$	$R_1 = 0.0375, wR_2 = 0.0859$
R indices (all data)	$R_1 = 0.0558, wR_2 = 0.1296$	$R_1 = 0.0490, wR_2 = 0.0908$
Largest difference peak and hole ($e \text{ \AA}^{-3}$)	1.455 and -0.538	0.418 and -0.218

Table 3
Comparison of selected bond lengths (Å) and bond angles (°) of Hdptsc, [Cu(dptsc)Br]₂ and [Cu(dptsc)(N₃)₂]

	Hdptsc	[Cu(dptsc)Br] ₂	[Cu(dptsc)(N ₃) ₂]
S(1)–C(12)	1.668	1.721	1.744
N(3)–C(6)	1.295	1.298	1.299
N(3)–N(4)	1.361	1.354	1.370
N(4)–C(12)	1.377	1.343	1.326
N(5)–C(12)	1.350	1.344	1.354
Cu(1)–S(1)		2.2565	2.2603
Cu(1)–N(1)		2.019	2.027
Cu(1)–N(3)		1.979	1.964
Cu(1)–N(2)		2.352	
Cu(1)–Br(1)		2.4134	
Cu(1)–N(6)			1.9561
Cu(1)–N(6)a			2.5628
C(6)–N(3)–N(4)	120.87	118.9	120.36
N(3)–N(4)–C(12)	118.72	111.1	111.68
N(5)–C(12)–N(4)	113.74	115.6	115.02
N(5)–C(12)–S(1)	123.48	118.9	119.09
N(4)–C(12)–S(1)	122.77	125.4	124.89
N(1)–Cu(1)–N(3)		80.05	80.56
S(1)–Cu(1)–N(1)		163.28	160.88
S(1)–Cu(1)–N(3)		83.60	84.95
S(1)–Cu(1)–N(2)		100.88	
N(2)–Cu(1)–N(1)		89.00	
N(2)–Cu(1)–N(3)		113.93	
Br(1)–Cu(1)–S(1)		95.22	
Br(1)–Cu(1)–N(1)		96.81	
Br(1)–Cu(1)–N(2)		97.60	
Br(1)–Cu(1)–N(3)		148.15	
S(1)–Cu(1)–N(6)			100.81
S(1)–Cu(1)–N(7)			81.74
S(1)–Cu(1)–N(6)a			104.53
N(1)–Cu(1)–N(6)			94.28
N(1)–Cu(1)–N(7)			112.12
N(1)–Cu(1)–N(6)a			87.77
N(3)–Cu(1)–N(6)			173.80
N(3)–Cu(1)–N(7)			166.63
N(3)–Cu(1)–N(6)a			89.29
N(6)–Cu(1)–N(7)			19.40
N(6)–Cu(1)–N(6)a			87.06
N(7)–Cu(1)–N(6)a			95.25
Cu(1)–N(6)–Cu(1)a			92.94

distance is found to be 2.5628 Å. The nitrogen atoms N(3) and N(6) are closer to the Cu(II) center with bond distances Cu(1)–N(3) (1.964 Å) and Cu(1)–N(6) (1.956 Å) compared to Cu(1)–N(1) (2.027 Å) and Cu(1)–S(1) (2.2603 Å). A maximum deviation of 0.1649 Å at N(1) is revealed at the base of the square pyramid with the central Cu(II) atom positioned 0.0689 Å above the mean plane. The pyridyl ring Cg(1) is less deviated from the basal plane (the dihedral angle between the two least square planes is 3.00°), when compared to the thiosemicarbazone moiety, which deviates more, at a dihedral angle of 13.51° from the basal CuN₃S plane. The dimer is located on an inversion centre and the bridging Cu₂N₂ network is perfectly planar. Similar to **2** above, the C(6)–N(3) and N(3)–N(4) bond

distances in **3** reveal extensive delocalization over the entire binuclear coordination framework.

The diverse π – π stacking, C–H... π and ring–metal interactions give rise to polymeric chains in the unit cells of **2** and **3** (Figs. 4 and 5). The shortest π – π interactions are perceived at 3.3631 Å for Cg(2)–Cg(2)ⁱ [$i = 1 - x, 1 - y, 1 - z$] in **2**. Ring–metal interactions Cg(2)–Cu(1)ⁱⁱⁱ [$iii = x, 1/2 - y, 1/2 + z$] are observed in **3** at a distance of 3.774 Å. Two C–H... π interactions each are shown in the unit cells of **2** and **3**. They are C(8)–H(8)–Cg(1)^{iv} [$d_{H...Cg} = 3.0853$ Å; $iv = -1 + x, y, z$] and C(10)–H(10)–Cg(5)^v [$d_{H...Cg} = 2.6471$ Å; $v = -1 + x, 1/2 - y, -1/2 + z$] for **2** and C(10)–H(10)–Cg(3)^{vi} [$d_{H...Cg} = 2.9888$ Å; $vi = 1 - x, -y, 1 - z$] and C(15)–H(15)–Cg(2)^{vii} [$d_{H...Cg} = 2.9537$ Å; $v = 1 - x, -1/2 + y, 1/2 - z$] for compound **3**.

3.3. Spectrochemical studies

The ν_a (N–H) vibrations of the imino group are observed at ca. 3428 cm^{–1} in the IR spectrum of Hdptsc. In the ¹H NMR spectrum, the N(4)H resonance, at a downfield value of 14.68 ppm, is consistent with the intramolecular N(4)–H...N(2) hydrogen bonding revealed by its crystal structure [30]. A strong band at 1580 cm^{–1} in the IR spectrum of Hdptsc corresponds to ν (N3–C6) stretching, which suffers a positive shift on complexation due to a change in bond order [31,32] (Table 4). The absence of a ν (S–H) band around 2565 cm^{–1} supports the predominant thione form of the ligand in the solid state, while the lack of an (N–H) stretching in the spectra of the complexes endorses the ligand coordination to Cu(II) ion in the deprotonated thiolate form. A medium band around 644 cm^{–1} indicates out-of-plane pyridyl ring vibrations ρ (py) of Hdptsc, which suffers a positive shift in all complexes. The IR bands observed at 1360 and 793 cm^{–1} in the ligand have significant contributions from C=S stretching and bending vibrations, and are shifted to lower wavenumbers on complexation [33]. Solid state reflectance spectrum of the ligand shows an absorption maximum in the region 37000 cm^{–1} attributed to intra-ligand $\pi^* \leftarrow \pi$ transitions of the pyridyl ring and imine function of the thiosemicarbazone moiety (Table 5). The peaks at ca. 27 000 and 30 030 cm^{–1} indicate $\pi^* \leftarrow n$ transitions of the thioamide function, which are shifted to higher energy values upon complexation. As expected, the Cu(II) \leftarrow S charge transfer transitions [34] are observed at ca. 23 000 cm^{–1}. For all the compounds, the peaks observed at ca. 17 000 and 14 000 cm^{–1} are assigned to d_{xz} , $d_{yz} \leftarrow d_{x^2-y^2}$ and $d_z^2 \leftarrow d_{x^2-y^2}$ transitions in an elongated square based pyramidal geometry [35,36]. Magnetic moment values for the bromo (**2**) and nitrate (**4**) complexes are greater than the spin only value for a dimeric system, since a larger Cu–Cu distance, revealed by the crystal structure in **2**, render the electron spins parallel resulting

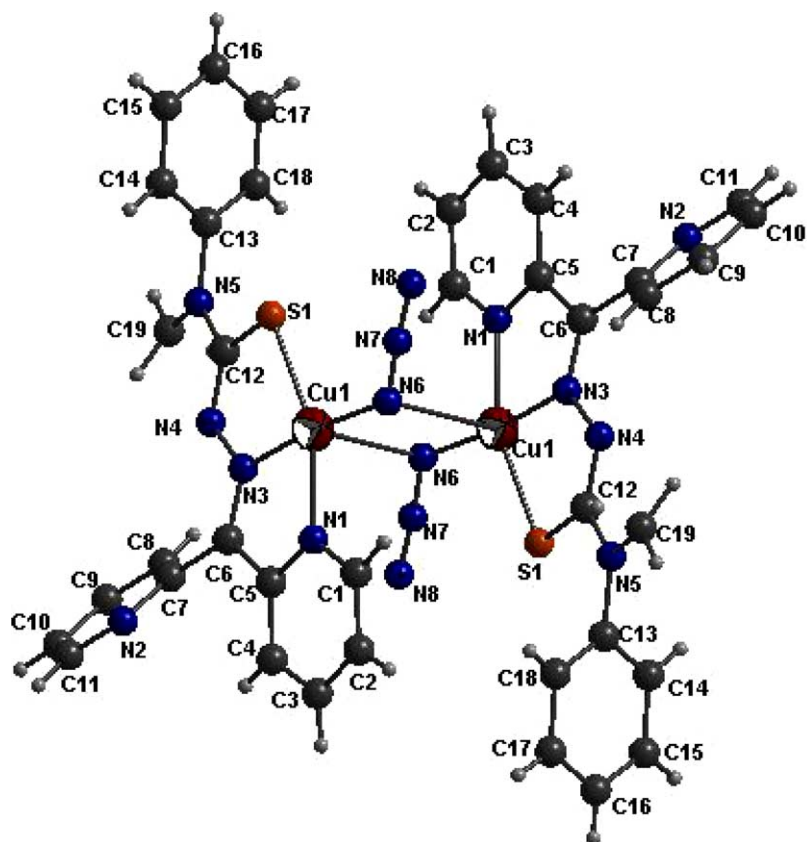


Fig. 3. Molecular structure of complex 3.

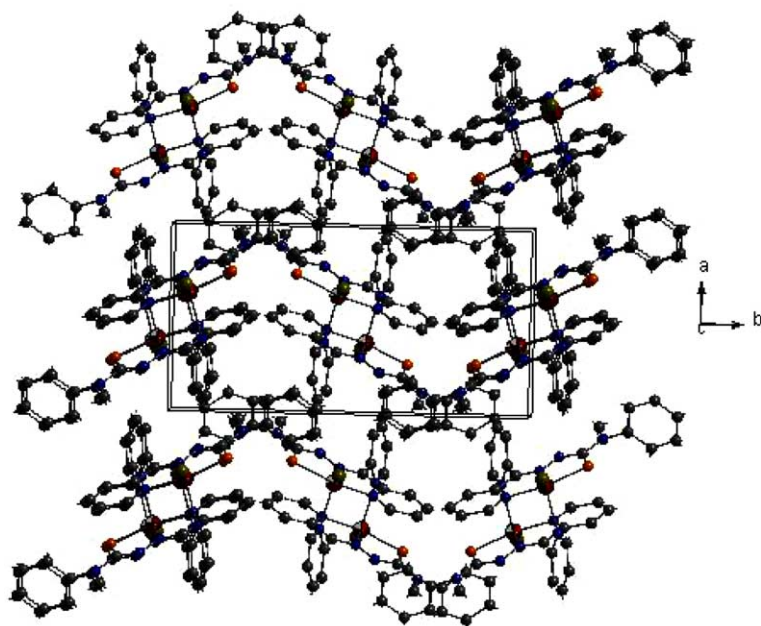


Fig. 4. Molecular packing diagram of 2 viewed down the 'c' axis.

in a high magnetic moment. The azido (3) and the chloro complex (1) show magnetic moment values close to the spin only value per copper for a dimer, suggesting the ab-

sence of spin-orbit coupling and anti-ferromagnetic interactions. A medium band at 245 cm^{-1} in the IR spectrum of 2 is indicative of the coordinated bromine.

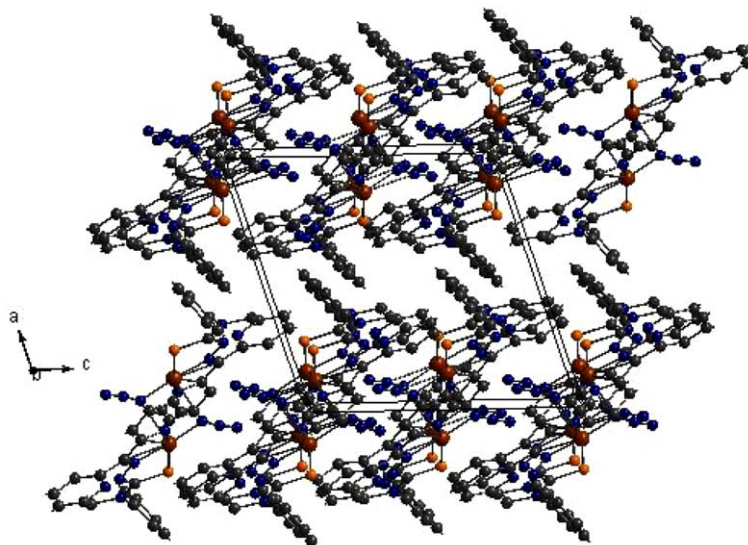


Fig. 5. Molecular packing diagram of **3** viewed down the 'b' axis.

Table 4
Selected IR bands (cm^{-1}) with tentative assignments for the complexes

Compound	$\nu(\text{C}=\text{N}) + \nu(\text{N}=\text{C})$	$\nu(\text{N}-\text{N})$	$\nu(\text{C}=\text{S})$	$\delta(\text{C}=\text{S})$	δ (o.p)	$\nu(\text{Cu}-\text{N})$	$\nu(\text{Cu}-\text{S})$	$\nu(\text{Cu}-\text{N})$ py	$\nu(\text{Cu}-\text{X}^{\#})$
Hdptsc	1580 s	1051 w	1360 s	793 m	644 m				
$[\text{Cu}(\text{dptsc})\text{Cl}]_2 \cdot 3\text{H}_2\text{O}$ (1)	1592 m	1004 w	1305 m	781 w	683 w	419 s	325 s	353 m	303 m
$[\text{Cu}(\text{dptsc})\text{Br}]_2$ (2)	1590 w	1002 w	1306 m	781 m	692 m	419 s	328 m	350 m	245 m
$[\text{Cu}(\text{dptsc})(\mu\text{-N}_3)]_2$ (3)	1594 m	1011 m	1310 sh	778 w	699 m	444 s	332 sh	351 m	315 m
$[\text{Cu}(\text{dptsc})(\text{NO}_3)]_2 \cdot \text{H}_2\text{O}$ (4)	1592 w	1005 m	1308 m	775 m	692 m	416 s	325 m	355 m	444 w

Table 5
Electronic spectral data (cm^{-1}) of Hdptsc and the complexes

Compound	d-d	C T	$\pi^* \leftarrow n$	$\pi^* \leftarrow \pi$
Hdptsc			26882 s, 30030 sh	37543 s, 32787 sh
$[\text{Cu}(\text{dptsc})\text{Cl}]_2 \cdot 3\text{H}_2\text{O}$ (1)	17636 sh, 14084 sh	24814 sh, 23201 s	32154 s 30395 b	37313 s
$[\text{Cu}(\text{dptsc})\text{Br}]_2$ (2)	17699 sh, 14556 sh	28169 sh, 23310 sh, 22831 s,b	32467 s, 31648 sh	37453 s
$[\text{Cu}(\text{dptsc})(\mu\text{-N}_3)]_2$ (3)	17211 sh, 144450 sh	26882 sh, 22676 s	32573 sh, 30864 sh	
$[\text{Cu}(\text{dptsc})(\text{NO}_3)]_2 \cdot \text{H}_2\text{O}$ (4)	17007 sh, 14104 sh	23095 s,b, 16949 sh	30487 s,b	38314 sh

Compound **3** exhibits strong bands at 2041 and 1310 cm^{-1} corresponding to the ν_a and ν_s of the coordinating azido group [37]. The prominent bands at 699 cm^{-1} and a weak band at 444 cm^{-1} , assigned to $\delta(\text{NNN})$ and $\nu(\text{Cu}-\text{N})$, suggest a non-linear Cu-N-N-N bond [34]. Bands corresponding to ν_1 , ν_2 , ν_4 at 1010, 1284 and 1385 cm^{-1} , respectively, are observed in **4**

whereas a $\nu_1 + \nu_4$ combination band at ca. 1750 cm^{-1} indicates monocoordinated nitrate group [37]. Magnetic moment measurement of **4** supports its potential dimeric disposition where the magnetic susceptibility value is found to be higher than that of a coupled Cu(II) ion pair, which is presumed with the association of small amounts of paramagnetic impurities in the compounds [38].

3.4. Electron paramagnetic resonance spectra

EPR spectra of the samples with 100-kHz field modulation at room temperature were recorded in the X-band. An isotropic spectrum with a broad signal is obtained for **3** and the remaining complexes gave axial spectra in the solid state at room temperature. The copper(II) ion, with a d^9 configuration, has an effective spin of $S = 1/2$ and is associated with a spin angular momentum $m_s = \pm 1/2$, leading to a doubly degenerate spin state in the absence of a magnetic field. In a magnetic field the degeneracy is lifted between these states and the energy difference between them is given by $E = h\nu = g\beta H$, where h is Planck's constant, ν is the frequency, g is the Lande's splitting factor (equal to 2.0023 for a free electron), β is the Bohr magneton and H is the magnetic field. For the case of a $3d^9$ copper(II) ion, the appropriate spin Hamiltonian assuming a B_{1g} ground state [36] is given by:

$$\hat{H} = \beta[g_{\parallel}H_zS_z + g_{\perp}(H_xS_x + H_yS_y)] + A_{\parallel}I_zS_z + A_{\perp}(I_xS_x + I_yS_y)$$

The EPR spectra of the compounds **1**, **2** and **4** in the polycrystalline state at 298 K show typical axial spectra with slightly different g_{\parallel} and g_{\perp} features. The variations in g values indicate that the geometry of the compound is affected by the nature of the coordinating ligands (Table 6). The spectrum of compound **3** in the polycrystalline state (298 K) shows a broad signal indicating only one g value, 2.0638, due to dipolar broadening and enhanced spin lattice relaxation.

The geometric parameter G calculated as $G = (g_{\parallel} - 2.003)/(g_{\perp} - 2.003)$ is a measure of the exchange interaction between copper centers in the polycrystalline compound. It is perceived that, if $G > 4$, the exchange interaction is negligible and vice versa in the complexes. All complexes with $g_{\parallel} > g_{\perp} > 2.003$ and G values falling within the range of 2–4 are consistent with a $d_{x^2-y^2}$ ground state in a square planar or square pyramidal geometry. The g values are found to be lower than those reported for copper(II) complexes prepared from a substituted 2-benzoylpyridine thiosemicarbazone [39], indicating a stronger metal-ligand bonding. Absence of half field signals for the compounds reinforces the assumption of very weak super exchange interactions.

The solution spectra of complexes **1** and **4** were recorded in DMF at 298 K. They are isotropic in nature with well-resolved four hyperfine lines. The hyperfine splitting is due to the interaction of the electron spin with the copper nuclear spin (^{65}Cu , $I = 3/2$). There are indications of nitrogen superhyperfine splitting in the high field component in some spectra. The A_{iso} and g_{iso} values show variations in **1** and **4**, their values indicating dissimilarity in bonding in the complexes.

The spectra of complexes **1**, **3** and **4** in DMF at 77 K show rhombic features with three g values g_1 , g_2 , and g_3 where $g_3 > g_2 > g_1$. It is observed that the g values for complexes in the solid state at 298 K and in DMF at 77 K are not much different from each other, hence the geometry around the copper(II) ion is unaffected on cooling the solution to liquid nitrogen temperature. In the low field region, the chloro and nitrate complexes show six hyperfine lines that are moderately resolved and perpendicular features overlapping with seventh one suggesting a dimeric state with two copper centers. The g_3 values of the complexes are less than 2.3 and they assign considerable covalent character to the M–L bonds [40]. For the compounds **1**, **3** and **4**, the lowest g value (g_1) is less than 2.04 indicating a compressed rhombic symmetry with all axes aligned parallel and is consistent with distorted trigonal bipyramidal stereochemistry or a compressed axial symmetry or rhombic symmetry with slight misalignment of the axes. In the spectra with $g_3 > g_2 > g_1$, rhombic spectral values $R = (g_2 - g_1)/(g_3 - g_2)$ may be significant. If $R > 1$, a predominant d_{z^2} ground state is present. If $R < 1$, a predominant $d_{x^2-y^2}$ ground state is present and when $R = 1$, then the ground state is approximately an equal mixture of d_{z^2} and $d_{x^2-y^2}$, the structure is intermediate between square planar and trigonal bipyramidal geometries. All the present complexes have values $R < 1$ suggesting a distorted square based pyramidal geometry with a $d_{x^2-y^2}$ ground state. These observations are consistent with g values of the corresponding complexes in the polycrystalline state at 298 K and further supports the distorted square pyramidal geometry around copper(II) ion in these complexes.

Spin Hamiltonian parameters are calculated from the frozen state EPR and electronic spectra (Table 7). The

Table 6
EPR spectral assignments (experimental) for the copper(II) complexes

Compound	Solid (298 K)			DMF(298 K)			DMF (77 K)					
	g_{\parallel}	g_{iso}	g_{\perp}	g_{iso}	A_{iso}	A_N	g_3/g_{\parallel}	g_2	g_1/g_{\perp}	g_{av}	A_{\parallel}^a	$A_{\perp}(N)^a$
[Cu(dptsc)Cl] ₂ · 3H ₂ O (1)	2.1422		2.0576	2.0446	43.33	15	2.2224	2.0597	1.9808	2.0876	63.33	11.66
[Cu(dptsc)Br] ₂ (2)	2.1349		2.0602				2.1423		2.0612	2.0882		
[Cu(dptsc)(μ-N ₃) ₂ (3)		2.0638					2.1961	2.0631	1.9868	2.0820	175	22
[Cu(dptsc)(NO ₃) ₂ · H ₂ O (4)	2.1484		2.0384	2.1047	48.33	20	2.1816	2.0341	1.9723	2.0627		

^a A values in 10^{-4} cm^{-1} .

Table 7

Spin Hamiltonian and orbital reduction parameters of the complexes **1** and **4**

Compound	[Cu(dptsc)Cl] ₂ · 3H ₂ O (1)	[Cu(dptsc)(NO ₃) ₂ · H ₂ O (4)
$g_{\parallel/gzz}(g_3)$	2.2224	2.1816
$g_{yy}(g_2)$	2.0597	2.0341
$g_{xx}(g_1)$	1.9808	1.9723
g_{av} (77k)	2.0876	2.0627
g_{av} (solid)	2.0858	2.0750
R^a	0.404	0.98
K_{\parallel}	0.6686	0.6357
K_{\perp}	0.6534	0.6030

$$^a R = (g_2 - g_1)/(g_3 - g_2).$$

orbital reduction factors were estimated using the following expressions [41].

$$K_{\parallel}^2 = (g_{\parallel} - 2.0023)\Delta E(d_{xy} - d_{x^2-y^2})/8\lambda_0,$$

$$K_{\perp}^2 = (g_{\perp} - 2.0023)\Delta E(d_{xz,yz} - d_{x^2-y^2})/2\lambda_0,$$

where λ_0 is the spin-orbit coupling constant and has a value of -828 cm^{-1} for Cu(II) d^9 systems.

According to Hathaway [42], $K_{\parallel} = K_{\perp} = 0.77$ for pure σ bonding and $K_{\parallel} < K_{\perp}$ for in-plane bonding, while for out-of-plane bonding $K_{\parallel} > K_{\perp}$. It is seen that for complexes **1** and **4** $K_{\parallel} > K_{\perp}$, indicating stronger out-of-plane π bonding.

4. Supplementary data

Crystallographic data for structural analysis has been deposited with the Cambridge Crystallographic Data center, CCDC 231110 for compound [Cu₂(dptsc)₂Br₂] (**2**) and CCDC 231109 for compound [Cu₂(dptsc)₂(N₃)₂] (**3**). Copies of this information may be obtained free of charge from The Director, CCDC, 12 Union Road, Cambridge, CB2 IEZ, UK (fax: +44-1223-336-033; e-mail: deposit@ccdc.cam.ac.uk or <http://www.ccdc.cam.ac.uk>).

Acknowledgements

The authors are thankful to the Regional Sophisticated Instrumentation Center, CDRI, Lucknow, India, for the elemental analysis and Sophisticated Instruments Facility, IISc Bangalore for NMR measurements.

References

- [1] S.P.J. Albracht, *Biochim. Biophys. Acta* 111 (1993) 317.
- [2] D.L. Klayman, J.P. Scovill, J.F. Bartosevich, J. Bruce, *J. Med. Chem.* 26 (1983) 35, and references therein.
- [3] G.Z. Bahr, *Allg. Chem.* 268 (1952) 351A.
- [4] G.Z. Bahr, *Allg. Chem.* 273 (1952) 325A.
- [5] A.G. Quiroga, J.M. Perez, E.I. Montero, D.X. West, C. Alonso, C.N. Ranninger, *J. Inorg. Biochem.* 75 (1999) 293.
- [6] F.A. French, E.J. Blanz Jr., *J. Med. Chem.* 9 (1996) 585.
- [7] A.S. Dobek, D.L. Klayman, E.T. Dickson, J.P. Scovill, E.C. Tramont, *Antimicrob. Agents Chemother.* 18 (1980) 27.
- [8] D.L. Klayman, A.J. Lin, J.W. McCall, *J. Med. Chem.* 34 (1991) 1422.
- [9] C. Shipman Jr., H. Smith, J.C. Drach, D.L. Klayman, *Antiviral Res.* 6 (1986) 197.
- [10] P.J. Blower, T.C. Castle, A.R. Cowley, J.R. Dilworth, P.S. Donnelly, E. Labisbal, F.E. Sowrey, S.J. Teat, M.J. Went, *J. Chem. Soc., Dalton Trans.* (2003) 4416.
- [11] R.I. Maurer, P.J. Blower, J.R. Dilworth, C.A. Reynolds, Y. Zheng, G.E.D. Mullen, *J. Med. Chem.* 45 (2002) 1420.
- [12] P. Bindu, M.R.P. Kurup, T.R. Satyakeerthy, *Polyhedron* 18 (1999) 321.
- [13] R.P. John, A. Sreekanth, M.R.P. Kurup, A. Usman, I.A. Razak, H.K. Fun, *Spectrochim. Acta* 59A (2003) 1349.
- [14] M.R.P. Kurup, M. Joseph, *Synth. React. Inorg. Met.-Org. Chem.* 33 (2003) 1275.
- [15] A. Sreekanth, S. Sivakumar, M.R.P. Kurup, *J. Mol. Struct.* 655 (2003) 47.
- [16] A. Sreekanth, U.L. Kala, C.R. Nayar, M.R.P. Kurup, *Polyhedron* 23 (2004) 41.
- [17] A. Sreekanth, M.R.P. Kurup, *Polyhedron* 23 (2004) 969.
- [18] C. Duan, B. Wu, T.C. Mak, *J. Chem. Soc., Dalton Trans.* (1996) 3485.
- [19] C. Duan, X. You, T.C. Mak, *Acta Crystallogr.* C54 (1935) 1935.
- [20] C. Duan, X. You, T.C. Mak, *Acta Crystallogr.* C54 (1935) 1937.
- [21] J.K. Swearingen, D.X. West, *Transition Met. Chem.* 26 (2001) 252.
- [22] J.K. Swearingen, W. Kaminsky, D.X. West, *Transition Met. Chem.* 27 (2002) 724.
- [23] A. Usman, I.A. Razak, S. Chantrapromma, H.K. Fun, V. Philip, A. Sreekanth, M.R.P. Kurup, *Acta Crystallogr.* C58 (2002) 0652.
- [24] V. Philip, V. Suni, M.R.P. Kurup, M. Nethaji, *Polyhedron* 23 (2004) 1225.
- [25] Siemens, SMART and SAINT, Area Detector Control and Integration Software, Siemens Analytical X-ray Instruments Inc., Madison, Wisconsin, USA, 1996.
- [26] G.M. Sheldrick, *Acta Crystallogr.* A46 (1990) 467.
- [27] G.M. Sheldrick, SHELXS-97 Program for the Solution of Crystal Structures, University of Göttingen, Göttingen, Germany, 1997.
- [28] K. Brandenburg, H. Putz, DIAMOND version 3.0, Crystal Impact, GbR, Postfach 1251, D-53002 Bonn, Germany, 2004.
- [29] B.N. Figgis, *Introduction to Ligand Field*, Wiley Interscience, New York, 1976.
- [30] V. Philip, V. Suni, M.R.P. Kurup, *Acta Crystallogr.* C60 (2004) o856.
- [31] B.S. Garg, M.R.P. Kurup, S.K. Jain, Y.K. Bhoon, *Transition Met. Chem.* 16 (1991) 111.
- [32] M.J.M. Campbell, *Coord. Chem. Rev.* 15 (1975) 279.
- [33] R. Mayer, in: M. Jansen (Ed.), *Organosulfur Chemistry*, Interscience, New York, 1967.
- [34] R.P. John, A. Sreekanth, M.R.P. Kurup, S.M. Mobin, *Polyhedron* 21 (2002) 2515.
- [35] B.J. Hathaway, A.A.G. Tomlinson, *Coord. Chem. Rev.* 5 (1970) 24.

- [36] M.A. Ali, M.T.H. Tarafdar, *J. Inorg. Nucl. Chem.* 39 (1977) 1785.
- [37] K. Nakamoto, *Infrared and Raman Spectra of Inorganic and Coordination Compounds*, 5th ed., Wiley, New York, 1997.
- [38] Y. Journaux, J. Sletten, O. Kahn, *Inorg. Chem.* 24 (1985) 4063.
- [39] A. Sreekanth, M.R.P. Kurup, *Polyhedron* 22 (2003) 3321.
- [40] D. Kivelson, R. Neiman, *J. Chem. Phys.* 35 (1961) 149.
- [41] K.D. Karlin, J. Zubieta, *Copper Coordination Chemistry – Biological and Inorganic Perspectives*, Adenine Press, New York, 1983.
- [42] B.J. Hathaway, G. Wilkinson, R.D. Gillard, J.A. McCleverty (Eds.), *Comprehensive Coordination Chemistry*, Pergamon, Oxford, 1987.